REPORT DOCUMENTATION PAGE

FORM APPROVED
OMB No. 0704-0188

1. AGENCY USE ONLY *(Leave blank)*	2. REPORT DATE	3. REPORT TYPE AND DATES COVERED
	Sept. - Oct. 1997	Conference Paper

4. TITLE AND SUBTITLE

Design and Development of a Dynamically Deforming Leading Edge Airfoil for Unsteady Flow Control

5. FUNDING NUMBERS

ARO mIPR 133-94

6. AUTHOR(S)

M.S. Chandrasekhara, L.W. Carr, M.C. Wilder, G.N. Paulson, C.D. Sticht

7. PERFORMING ORGANIZATION NAME(S) AND ADDRESS(ES)

Navy-NASA Joint Institute of Aeronautics. Code AA/CH
Dept. of Aeronautics and Astronautics
Naval Postgraduate School, Monterey, CA 93943

8. PERFORMING ORGANIZATION REPORT NUMBER

9. SPONSORING/MONITORING AGENCY NAME(S) AND ADDRESS(ES)

U. S. Army Research Office
P.O. Box 12211
Research Triangle Park, NC 27709-2211

10. SPONSORING/MONITORING AGENCY REPORT NUMBER

ARO 32480.11-EG

11. SUPPLEMENTARY NOTES

The view, opinions and/or findings contained in this report are those of the author(s) and should not be construed as an official Department of the Army position, policy, or decision, unless so designated by other documentation.

12a. DISTRIBUTION/AVAILABILITY STATEMENT

Approved for public release; distribution unlimited.

12b. DISTRIBUTION CODE

13. ABSTRACT *(Maximum 200 words)*

A novel approach to unsteady flow separation and dynamic stall control using a dynamically deforming leading edge airfoil is described. The design details of a carbon-fiber composite skin airfoil having a thickness of 0.002 in. at the leading edge and capable of deforming at 20 Hz in unsteady flow at freestream Mach numbers of up to 0.45, are discussed. Implementation of the scheme at model scales places extraordinary demands on the design, material and fabrication of such an airfoil. Rate scaling further requires very-rapid-response instrumentat ion, measurement techniques and data acquisition schemes. The special instrumentation control system developed for these experiments as well as the fluid dynamic results of successful flow control that was achieved using this method, are also discussed.

14. SUBJECT TERMS

Composit Materials, Stall Control Airfoil Design

15. NUMBER OF PAGES

9

16. PRICE CODE

17. SECURITY CLASSIFICATION OF REPORT	18. SECURITY CLASSIFICATION OF THIS PAGE	19. SECURITY CLASSIFICATION OF ABSTRACT	20. LIMITATION OF ABSTRACT
UNCLASSIFIED	UNCLASSIFIED	UNCLASSIFIED	UL

DESIGN AND DEVELOPMENT OF A DYNAMICALLY DEFORMING LEADING EDGE AIRFOIL FOR UNSTEADY FLOW CONTROL

M.S. Chandrasekhara
Navy-NASA Joint Institute of Aeronautics, Department of Aeronautics and Astronautics
Naval Postgraduate School, Monterey, CA 93943

L.W. Carr
Aeroflightdynamics Directorate, U.S.Army ATCOM and,
Fluid Mechanics Laboratory Branch
NASA Ames Research Center, Moffett Field, CA 94035-1000

M.C. Wilder
MCAT Inc., San Jose, CA

G.N.Paulson and C.D.Sticht
NASA Ames Research Center, Moffett Field, CA 94035-1000

ABSTRACT

A novel approach to unsteady flow separation and dynamic stall control using a dynamically deforming leading edge airfoil is described. The design details of a carbon-fiber composite skin airfoil having a thickness of 0.002 in at the leading edge and capable of deforming at 20 Hz in unsteady flow at freestream Mach numbers of up to 0.45, are discussed. Implementation of the scheme at model scales places extraordinary demands on the design, material and fabrication of such an airfoil. Rate scaling further requires very-rapid-response instrumentation, measurement techniques and data acquisition schemes. The special instrumentation control system developed for these experiments as well as the fluid dynamic results of successful flow control that was achieved using this method, are also discussed.

1. INTRODUCTION

Ongoing research into compressibility effects on dynamic stall has shown that the primary cause of dynamic stall onset is the presence of a strong adverse pressure gradient near the airfoil leading edge and a combination of local supersonic flow causing shocks in this same region. These effects are induced by the sharp leading edge required for high speed performance and operation of a helicopter rotor blade on its advancing side. The sharp leading edge of the blade causes rapid acceleration of the air as it moves from the stagnation point to the suction peak located on the upper surface just downstream of the airfoil nose. The acceleration is fixed primarily by the nose curvature for a given set of flow conditions. As a helicopter or an aircraft executes a rapid maneuver, it produces a very high suction peak, as well as local supersonic flow conditions on the surface of the blade or wing and flow separation results. In the unsteady environment of the helicopter rotor this results in dynamic stall conditions, the avoidance of which severely limits the performance of the helicopter. There is a critical need to remove this limitation if an extension of the flight envelope is to be made possible. New airfoil concepts are required which do not suffer from the limitations of fixed geometry and can continuously adapt to dynamically changing flow conditions. The rapidly evolving field of smart materials offers significant potential for breakthroughs in this area.

The aerodynamic characteristics of such adaptive airfoils and wings must be determined precisely, which requires simulation of the appropriate and relevant geometry changes in the laboratory. Manipulating airfoil geometries at model scale (20:1) immediately leads to many engineering design challenges and places extraordinary demands on material properties used in airfoil construction. The requirement for phase locking the airfoil shape to the varying flow conditions over an airfoil oscillating at 20 Hz makes the task even more difficult. This paper provides details of a new wing design where a dramatic and effective flow control capability is introduced through small displacements of the airfoil leading edge. As much as six degrees of steady flow separation delay (relative to the static stall angle of a NACA 0012 airfoil) can be realized from the design. Even separated flow can be reattached by selectively deforming the airfoil leading edge.

The design philosophy followed for achieving effective flow control is: relative to that of the fixed geometry airfoil,

1. reduce the suction peak pressures for a given condition
2. reduce the strong adverse pressure gradient
3. distribute the low pressure region over a wider region of the upper surface in order to improve the airfoil performance.

It is difficult to produce dynamic deformation of the airfoil surface at the rates needed in the present application. As part of the investigation of methods for driving the surface, a variety of mechanisms were considered. Analysis showed that pneumatic deicing boots were too slow to meet model scale response rates. An electro-expulsive technique developed at NASA Ames Research Center(ARC) was evaluated, but it produced highly three-dimensional deformation that was unacceptable for the present application. After consideration of several such concepts it was concluded that a mechanical drive offered the best control over position, phase, amplitude and rate changes of the

deformation of the airfoil leading edge.

The major design considerations were: the force required to produce the desired deformation at rapid rates in the unsteady flow under investigation (oscillating airfoil flow at a freestream Mach number of up to 0.45 and frequencies of 20 Hz); the material fatigue properties; the continuity of slope and curvature of the airfoil surfaces; and the fabrication effort required. The final choice was a design consisting of a carbon-fiber composite skin for the airfoil surface from the leading edge up to the 0.2c location, with a mandrel housed inside between the airfoil upper and lower surfaces. The mandrel, attached to the skin at the leading edge by a tang, is used to bring about the required deformation schedule, (Fig. 1 [1]). The rest of the airfoil was made from solid metal. The design aspects, the fabrication details, the control system, the data acquisition details and some representative results of the Dynamically Deforming Leading Edge(DDLE) airfoil flow are described below.

2. DETAILS OF DDLE AIRFOIL DESIGN, FABRICATION AND CONTROL SYSTEM

2.1. DESIGN SPECIFICATIONS

The following are the minimum design specifications for the DDLE airfoil:

1. The fully deformed airfoil is a 6 in chord, NACA 0012 airfoil.
2. The DDLE airfoil skin should withstand the very high suction levels ($C_p = -7.0$ at M = 0.3 near its leading edge) to which it is subjected as well as the local supersonic flow that occurs.
3. The airfoil should also withstand the aerodynamic loading in the freestream Mach number range from 0 to 0.45, and the oscillation frequency variation from 0 to 20 Hz for sinusoidal angle of attack variations of
$$\alpha = \alpha_0 + 10^0 \sin \omega t$$
with $\alpha_{0_{max}} = 15$ deg.
4. The airfoil nose curvature is to be changed from that of the 6 in chord NACA 0012 airfoil to a fully rounded leading edge airfoil. The specified deformation translates to a 320% change in curvature (from 0.095 in radius to 0.30 in radius). This requires a maximum leading edge retraction of 0.08 in. The rate of leading edge movement is programmable, with the fastest rates specified to occur in 10 ms, i.e. within one-quarter cycle of motion on the airfoil upstroke. After a dwell time the leading edge is returned to its original NACA 0012 profile, which is maintained for the rest of the cycle. However, both the actual displacement and the duty cycle are required to be fully controllable, up to a maximum frequency of 20 Hz.
5. The design shall fit in the existing windows of the 10 in X 14 in Compressible Dynamic Stall Facility (CDSF).

In order to minimize the power requirements of the drive system used to actuate the airfoil leading edge, it was necessary to conceive a design consisting of a very thin layer of composite material - 0.002 in - at the airfoil nose. To provide the necessary strength from aerodynamic and material fatigue considerations the skin thickness increased in sections.

2.2. DESIGN DETAILS

The 6-inch chord DDLE airfoil model is made in two sections with the first 20% of the chord from a carbon fiber composite material and the rest from solid aluminum. Selection of the leading edge material was based on yield strength with the requirement of maintaining the deformed NACA 0012 shape with and without aerodynamic loads while minimizing the actuator loads. A study of materials available in sheet form was conducted in order to determine the feasibility of designing and fabricating the DDLE airfoil completely from metal. The use of metals was precluded by the fact that all metals either yielded when formed to the required radius or were too thin to support the structural and aerodynamic loads that occurred. There were additional problems that needed to be addressed if metals were to be used: the excessively thin sections needed to reduce levels of stress, heat treating very thin wing skins (that causes warpage), chemical milling to vary thickness, residual stress from forming a sheet and large driving loads, etc. These concerns all led to the selection of a composite material for the present application.

A particular advantage of using a composite material is that it allows for tailoring of the wing skin thickness and stiffness. Among the limitations of using composite material is the availability of small ply thickness (with the current design requiring 0.001 inch). The leading edge skin is fabricated from a fiber glass and carbon fiber unidirectional tape with an ultimate tensile strength of 2.3×10^5 psi and a modulus of elasticity of 1.9×10^7 psi for the carbon fiber. The ply lay-up is symmetric and the nose is fabricated from 2-plys of fiberglass laid at 0 deg. The skin thickness increases aft of the nose up to 0.025 in (25-plys) with the plys laid in the pattern of the four layers at ± 30 deg and the following two layers at 0 deg and so on. This alternating pattern was used for strength reasons. The thickness reduces to 0.009 in near the point where the deforming section is attached to the main airfoil as shown in Fig. 1.

The composite material design was first tested through a computer simulation and the construction of an oversized bench-test model. A NASTRAN finite element computer code was used to study the shape of the deformed leading edge, the material stresses and driving loads. The design is nonlinear due to internal contact of the skin on the driving push plate; which is required to shape the leading edge to the NACA 0012 contour. This contact is represented with a so-called GAP element which transfers load when the gap between adjacent parts is closed. A 5-times scale bench-test model was fabricated to study loads and the deformed shape relative to the ideal NACA 0012 airfoil. As can be seen in Fig. 2, the NASTRAN model simulation and the bench-test showed good correlation for loads causing up to 0.25 in deformation. However, at a chordwise deflection of 0.375 in the NASTRAN model over predicted the load by 36%. Beyond a deformation of 0.25 in the composite leading edge loading *vs* displacement was highly nonlinear as noted above.

The drive mechanism for the wind tunnel model consists of a slider-crank mechanism with a crank rotation through 14 degrees producing translational motion at the leading edge of 0.088 in. An internal push

plate having the shape of the NACA 0012 airfoil for 2.8% of the chord is used to force the airfoil surface to match the NACA 0012 shape when the push plate is fully extended. During the process the push plate contacts the skin producing a nonlinear driving force as a function of displacement. Energy stored in the leading edge skin when it is formed to the NACA 0012 shape is used to assist the drive system in returning the leading edge to the 0.3 in radius configuration. This reduces the load requirements of the drive system. Fig. 3 shows a schematic side view of the airfoil mounted in the CDSF test section windows and also the location of the motor drive system.

The DDLE drive system has been designed conservatively for flow conditions at M = 0.4 and a reduced frequency of 0.15. The maximum chordwise force at the peak stepper motor torque of 122 ft-lbs is 314 lbs of which the aerodynamic loads and stiffness in the skin together are 95 lbs. The total force required for a full leading edge displacement of 0.08 in under the less severe flow conditions at M = 0.3 and k = 0.05 is 145 lbs of which the aerodynamic load is 35 lbs. The total force increases to 182 lbs when the displacement is increased to 0.088 in for this lower speed flow condition. The maximum acceleration of the leading edge is about 33g. The skin is designed for a fatigue life of 140 hrs, with an adequate factor of safety. These extraordinary loads and rapid accelerations coupled with the extremely thin skin around the leading edge required a very tightly controlled drive system (described in Sec. 2.4).

2.3. FABRICATION OF THE DDLE SECTION

The DDLE surface was constructed using 0.001 in thick layers of fiber glass on the inside with carbon fiber material on the outside. At the nose of the airfoil (over the first 0.075 in) only a 2-ply fiber glass tape was used. More layers were added further along the airfoil surface with thickness varying as shown in Fig. 1. These layers were pre-impregnated with resin. A four-piece aluminum mold (two inner and two outer molds - see Fig. 4) were machined for curing the composite leading edge. The inner molds were intentionally undersized, with silicone rubber cast to the correct shape; the rubber was used to maintain pressure on the inner side of the composite skin while the material was cured in the mold. The material at the nose was sandwiched between the two inner molds to form a tang (used to hold the DDLE to the push plate), and then formed around the outside of the silicone rubber casting; this assembly was then put into the outer mold before curing.

In the first few attempts at fabricating the leading edge it was found that the carbon fiber unidirectional tape was too rigid to form around the tight (0.095 in) radius of the NACA 0012 airfoil when stretched. A variety of potential solutions were explored; the best option was then used for manufacturing the DDLE section, as follows. The carbon fiber sheets were assembled and compacted into two flat panels by evacuating the air between the layers, then joined to the inner mold. Once assembled, the unit was put into an oven at 175°F for two hours, allowing the resin to flow. The mold was then slowly closed, in order to not deform the fibers. After the closing process, which took two hours, the oven temperature was progressively raised over three hours to 270°F, held at 270°F for three hours, and then progressively decreased over five hours to 65°F. After curing, and before the part was removed from the molds, the aluminum strip used to attach the leading edge section to the main airfoil was positioned and bonded to the carbon fiber surface.

The carbon fiber DDLE skin was then attached to the push plate by sliding the tang into the slot already machined into the push plate. The tang was then bonded to the push plate by thermoset adhesive injected through ports in the push plate (thermoset adhesive was used to permit reuse of the push plate). The DDLE section was then attached to the main airfoil by screws.

2.4. MOTION ACTUATOR AND CONTROL SYSTEM

As stated above, the composite skin was attached with a tang to the drive mandrel which was shaped to the leading edge profile of a 6 in chord, NACA 0012 airfoil. The mandrel is linked to a truss, which is in turn connected to a drive motor on each end trough push rods. The DDLE motors are 2.1 hp brushless servo-stepper motors capable of intermittent operations through rapid, short angular motion. The motors are equipped with a 4096 steps/rev resolver with an accuracy of ±7 arc min. An encoder with 5400 counts/rev is mounted on the motor shaft to provide a digital display of the leading edge position. The motors are software driven from a PC through controllers which provide the ability to hold the DDLE at any predetermined position for as long as required for accomplishing detailed flow studies. It is possible to move the DDLE at different speeds through a range of positions or incrementally in minimum time to obtain a step change of shape. Fig. 5 shows the time history of motion obtained at different rates. It is clear that at the fastest rate, V(10), (where 10 denotes the highest rate parameter used in programming the drive system) the motion was completed in about 15ms, as designed. There is a minimum rise time of 3ms in all cases compared. The feed back control system is finely tuned to hold the airfoil shape against the wind load and to complete the required movements without introducing jitter during movement or oscillations at the ends of the duty schedule. The velocity and acceleration parameters of motion are carefully selected to achieve this goal.

A typical motion history consists of pushing the DDLE from a selectable relative home position to the most forward position (the NACA 0012 shape) where it is held until commanded to execute the desired deformation schedule at a pre-determined rate. The motion is phase locked to the desired airfoil angle of attack in its sinusoidal motion cycle as shown in the flow chart in Fig. 6. When a match occurs between the selected and actual angles of attack, a trigger pulse is issued by the Oscillating Airfoil Position Interface(OAPI) to the servomotor controller through a signal conditioner unit. The controller software (which is pre-loaded from the PC) is interrupt driven for phase locking purposes, with the interrupt pulse generated from the OAPI. The movement of the motors and thus of the DDLE is initiated by the controller following this event as shown in Fig. 6. A slightly varying time delay (attributable

to ongoing real-time processing within the PID loop) exists in the controller leading to some uncertainty (of the order of a few encoder counts) in phase locking. Presently this problem is being addressed, but success has been achieved by the simple solution of repeating the experiments.

3. DESCRIPTION OF THE EXPERIMENT

The experiments were conducted in the CDSF located at the Fluid Mechanics Laboratory of ARC. The CDSF, described completely in Carr and Chandrasekhara [2] is an in-draft wind tunnel with optical access for using nonintrusive flow diagnostic instrumentation. The DDLE airfoil is held between metal ports in the test section side walls which have 2 in X 4 in L-shaped optical glass window inserts. All load bearing components of the DDLE airfoil are supported in the metal portion of the windows. The 6 in chord airfoil is oscillated about the quarter-chord point, and the glass inserts provide a clear view of the leading 35% of the upper surface and about 20% of the lower surface.

The measurement technique used is the well established Point Diffraction Interferometry(PDI) technique described in Brock et al [3]. The PDI instrumentation uses a pulsed Nd-YAG laser for the light source with standard schlieren optics. The knife edge is replaced by a point diffractor, which is made from a partially developed, but unfixed photographic plate. A clear aperture is burned *in-situ* through the emulsion on the plate prior to starting the tunnel flow to serve as the point diffractor. Imaging optics are set up further downstream of the PDI plate to provide suitable image magnification.

Two different modes of PDI operation were used. In the first, still images were obtained for selected DDLE shapes at different angles of attack ranging from 6 - 20 deg and at different freestream Mach numbers from 0.2 to 0.45 in steady flow. In the second, PDI images of unsteady dynamic stall flow were recorded on a drum camera using the high speed, real time, phase locked PDI technique described in Chandrasekhara et al [4]. In the present application, an added complication was introduced due to two independent time dependent motions, namely, the sinusoidal oscillations of the airfoil and the DDLE shape changes at variable rates starting from an arbitrary airfoil angle of attack. This made the synchronization of the oscillating airfoil drive system, the DDLE motion controller, the high-speed camera and the pulsed laser a complex task. Fig. 6 shows the synchronization logic that was used. As stated earlier, the DDLE controller was interrupt driven by the matching OAPI TTL pulse. The movement of the DDLE was recorded using the encoder on the stepper motor shaft. Once motion was detected, the camera and laser synchronization were effected as was done in [4] for a fixed geometry airfoil. The high speed drum camera can record up to 224 images. In this study, 200 images/test condition were recorded at rates of up to 10 KHz. The DDLE was moved at different rates and starting at different angles of attack to document the flow over it and to establish the shape parameter range over which flow control could be achieved. The angles of attack (the airfoil encoder positions) were recorded in a FIFO buffer and were later downloaded into a μ-VAX II computer.

The interferograms were analyzed using software developed in-house on a work station [5].

4. RESULTS AND DISCUSSION

Of primary interest here is the range of shapes that could be generated with this design and the demonstration that the DDLE airfoil was effective in controlling flow separation. Bench tests were used to establish that the deformation was two-dimensional.

4.1. DDLE AIRFOIL SHAPES GENERATED

Figure 7 shows some of the shapes that were generated as the airfoil leading edge was retracted from the basic NACA 0012 profile position. The DDLE airfoil was subjected to the deformation under the no flow conditions and photographed at the PDI image plane. The images were digitized and, using an in-house developed package, the DDLE airfoil surface was traced to generate the profiles. In this context, a new airfoil shape is defined for each rearward leading edge displacement of 0.003 in from the previous position, with shape 0 being almost identical to the NACA 0012 shape. Fig. 7 shows the DDLE airfoil shapes 4, 9, 12 and 14 in addition to the NACA 0012 airfoil profile. Testing was carried out to shape 18, but for most practical purposes, the range of effective shapes is contained within the above four shapes. A major concern during the design was the continuity of airfoil surface curvature, which has a major influence on the flow. A slight discontinuity can be noticed at $x/c \approx 0.05$ for shape 4. This is attributed to the rigid constraint of continuous curvature and slope at the point where the solid airfoil is attached to the deforming skin. However, this point is sufficiently downstream of all major events in the flow to not be considered crucial to the flow development. Further, in the wind tunnel tests, the skin surface was covered with a continuous tape to smooth out any other manufacturing defects. It is believed that slight manufacturing imperfections will not adversely alter the flow development.

4.2. EFFECT OF AERODYNAMIC LOADING ON SHAPE CHANGE AND REPEATABILITY

Figure 8 shows the repetitions of a single setting for shape changes that were realized in three different motion histories in steady flow at M = 0.3 and α = 10 deg. Plotted on the ordinate are the DDLE shape numbers against time on the abscissa. In each case, the leading edge was retracted by 0.0626 in from the fully extended NACA 0012 shape at the maximum rate [V(10)] of the system. It is clear that the repeatability of the motion with time, and hence of shape, is excellent. Fig. 9 shows the effects of aerodynamic loading airfoil on shape history due to varying angle of attack at M = 0.3 in steady flow. Also shown is the no-flow case which takes the shortest time for a specified motion history since the feed back system is not working against any aerodynamic load. Interestingly, at α = 0 deg and at α = 18 deg, the deformation cycles coincide. It is believed that this is due to the fact that the feed back system is subjected to comparable

aerodynamic loading (the flow is fully stalled initially at an angle of attack of beyond 14 deg). The rate of movement is comparatively slower at $\alpha = 10$ deg due to the fact that the airfoil suction peak pressures are high and the resultant load on the drive system is high. However, as shown in Fig. 8, the motion repeats very well for each of these flow-on conditions. Repeatability tests showed that the maximum uncertainty was present for the 18 deg case and amounted to a displacement of less than 0.002 in (less than one-shape change).

Similar tests for the oscillating airfoil showed that the no flow oscillating deformation schedule agreed within the uncertainty of the experiment with the no-flow, no-oscillation schedule as shown in Fig. 10. With the airfoil aerodynamically loaded at M = 0.3 and oscillating at a reduced frequency of 0.05 (f = 10.8 Hz), a slightly delayed movement of the airfoil leading edge was observed. Since the angles of attack and the airfoil leading edge position are recorded simultaneously, these differences are not an issue.

4.3. FLOW OVER DIFFERENT SHAPES AT HIGH ANGLE OF ATTACK

Figure 11 presents PDI images of flow over different shapes in steady flow at M = 0.3 at an angle of attack of 18 deg. Earlier data [1] has shown that the static stall angle of attack for the NACA 0012 airfoil is about 14 deg. In Fig. 11a, the flow over shape 4 is still separated, however, as the airfoil leading edge is withdrawn another 0.015 in to shape 9, Fig. 11b, the flow can be seen to have fully reattached. It was also shown in Chandrasekhara et al [1] that reattachment begins before shape 8 is reached. The large number of fringes near the leading edge indicate the redevelopment of the suction peak from an originally separated flow and confirm that the flow can be forced to reattach by changing the leading edge curvature. In Fig. 11c, for shape 12, the flow is still attached with a laminar separation bubble over the upper surface. The suction peak is slightly lower than that seen in Fig. 11b as evidenced by the fewer fringes. In Fig. 11d fully separated flow is seen over shape 15. These results validate the ability of the DDLE concept to reattach a fully separated flow by changing the leading edge curvature through extremely small movement (0.02 - 0.04 in) of the leading edge.

Figure 12 shows a representative result for an unsteady flow case at M = 0.3, where the airfoil was oscillated at 10.8 Hz, with the airfoil shape fixed at shape 8. This shape had very favorable characteristics in steady flow up to $\alpha = 19$ deg. This figure was drawn by tracing the fringes in an image obtained using the high speed PDI technique. Several 200-image sequences having different starting angles of attack in order to document the flow behavior at all angles in the oscillation cycle were recorded. At 20 deg angle of attack, the fringe tracings show that the flow is still attached at the top of the oscillation cycle. In contrast to the flow over an oscillating NACA 0012 airfoil where the presence of a strong dynamic stall vortex was documented, there is no evidence of the dynamic stall vortex in this case, even at this high angle of attack. The dynamic stall vortex was also absent in all other images obtained in the tests.

5. CONCLUSIONS

A unique airfoil design has been created to control aerodynamic flow separation and dynamic stall under compressible conditions at rapid oscillation rates of up to 20 Hz. The design permits dramatic changes in the airfoil leading edge curvature to be realized through which the fluid acceleration can be carefully tailored to suit instantaneous flow conditions and maintain attached flow over the airfoil; even fully separated flow can be made to reattach. Complex instrumentation was developed for data acquisition by phase locking the high speed camera and pulsed laser with the motion of the DDLE, which was in turn phase locked to airfoil oscillations. Results presented demonstrate the significant success that was achieved in this unique experiment.

ACKNOWLEDGEMENTS

The project was supported by ARO-MIPR-96-7 to the Naval Postgraduate School and was monitored by T.L. Doligalski, with initial funding from AFOSR. Additional support was received from S.S. Davis, Fluid Mechanics Laboratory, NASA ARC. The expert advice of C.Hiel on composite fiber material fabrication, the DDLE control system design of D.D. Squires, and the help of R.A. Miller in model installation are all greatly appreciated.

6. REFERENCES

[1] M.S.Chandrasekhara, M.C.Wilder, and L.W.Carr, "Control of Flow Separation Using Adaptive Airfoils" *AIAA Paper No. 97-0655*, Reno, NV, Jan. 1997.

[2] Carr, L.W., and Chandrasekhara, M.S., "Design and Development of a Compressible Dynamic Stall Facility", *Journal of Aircraft*, Vol. 29, No. 3, pp. 314-318.

[3] N.Brock, M.S.Chandrasekhara, and L.W.Carr, "A Real Time Interferometry System for Unsteady Flow Measurements", ICIASF'91 RECORD, IEEE Publication 91-CH3028-8, pp. 423-430.

[4] M.S.Chandrasekhara, D.D.Squires, M.C.Wilder, and L.W.Carr, "A Phase Locked High Speed Real Time Interferometry System for Large Amplitude Unsteady Flows", *Experiments in Fluids*, Vol. 20, Dec. 1995, pp. 61-67.

[5] M.C.Wilder, M.S.Chandrasekhara, L.W.Carr, "Computer Aided Analysis of Interferometric Images of Unsteady Aerodynamic Flows", ICIASF'95 RECORD, IEEE Publication 95-CH3482-7, pp. 44.1 - 44.11.

[6] M.S.Chandrasekhara, M.C.Wilder, and L.W.Carr, "Unsteady Stall Control Using Dynamically Deforming Airfoils" *AIAA Paper No. 97-2236*, Atlanta, GA, Jun. 1997.

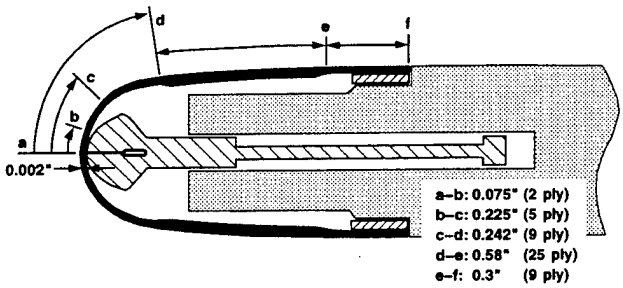

Fig. 1. Construction Details of the DDLE Airfoil Model.

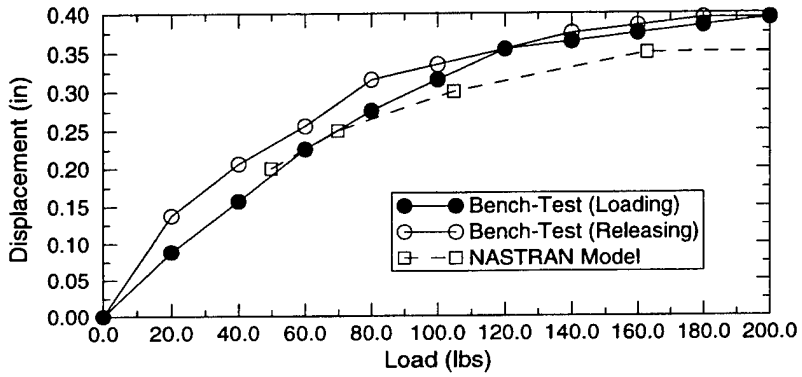

Fig. 2. Load vs. Displacement for the 5x Bench-Test and Simulation Models.

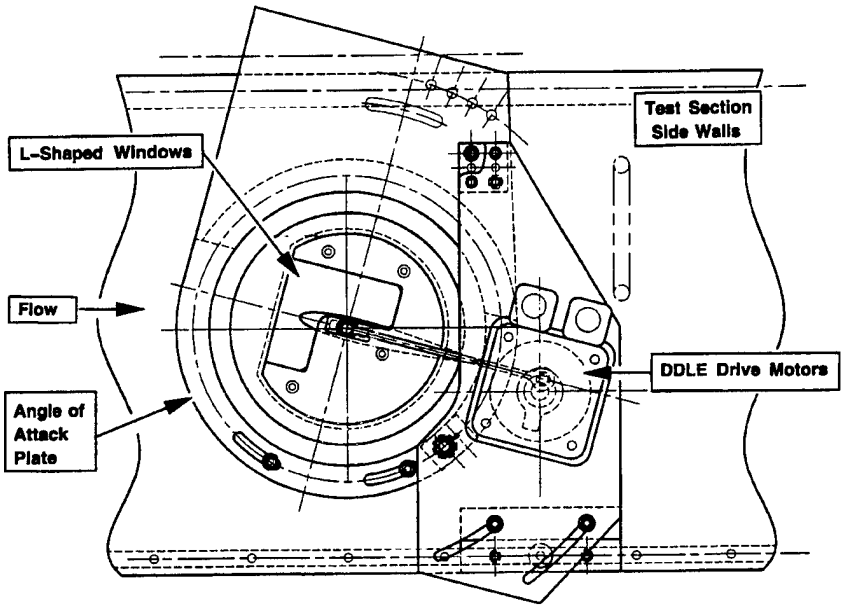

Fig. 3. Schematic of the DDLE Drive System on the Compressible Dynamic Stall Facility.

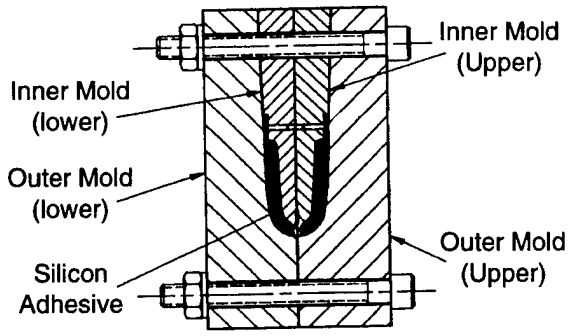

Fig. 4. DDLE Fabrication Mold

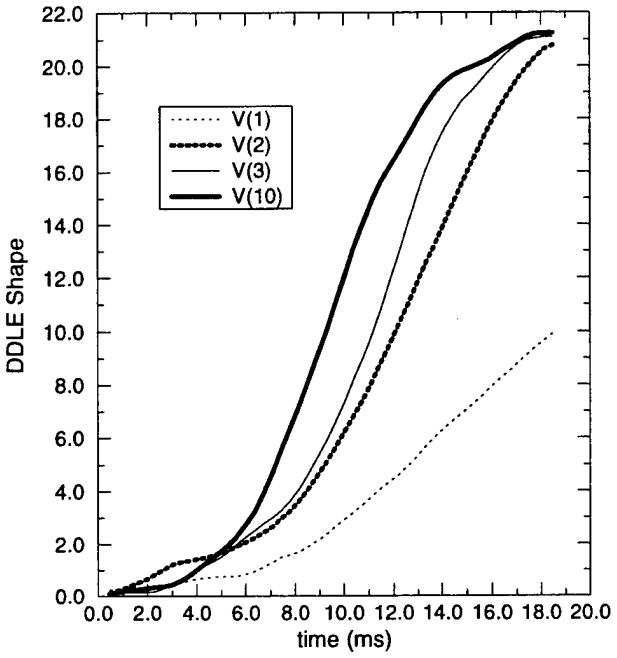

Fig. 5. DDLE Motion History for Different Rates, V.

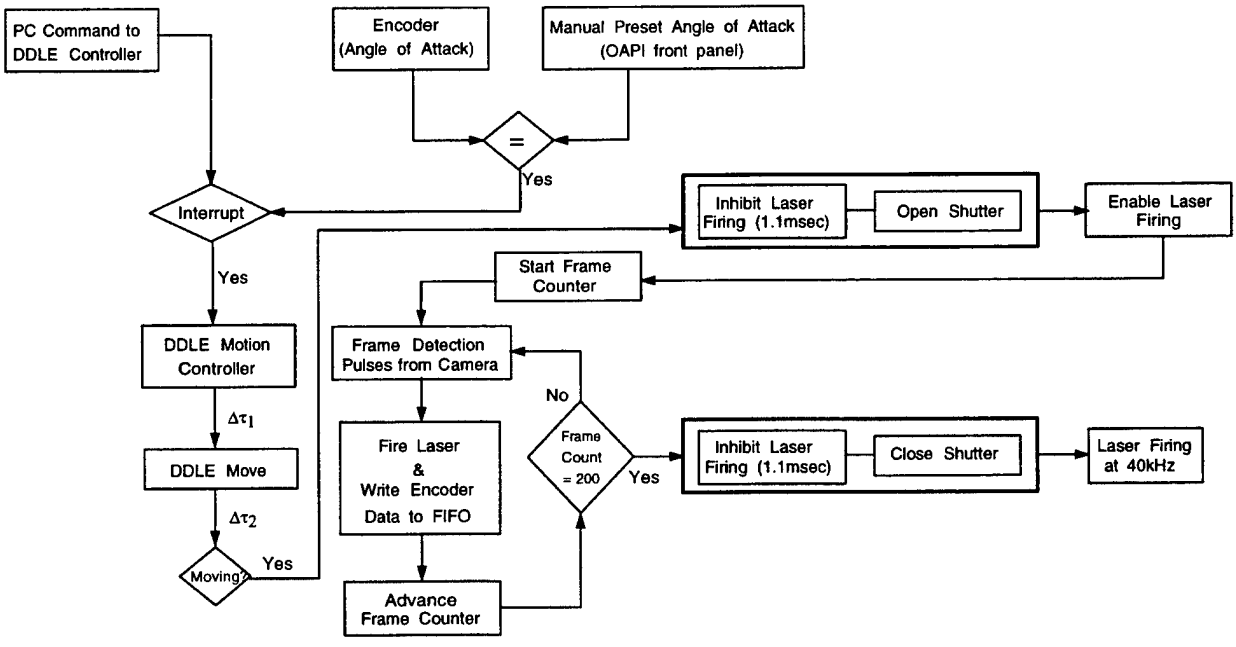

Fig. 6. Phase Interlocking of DDLE, CDSF, Pulsed Laser and High-Speed Camera.

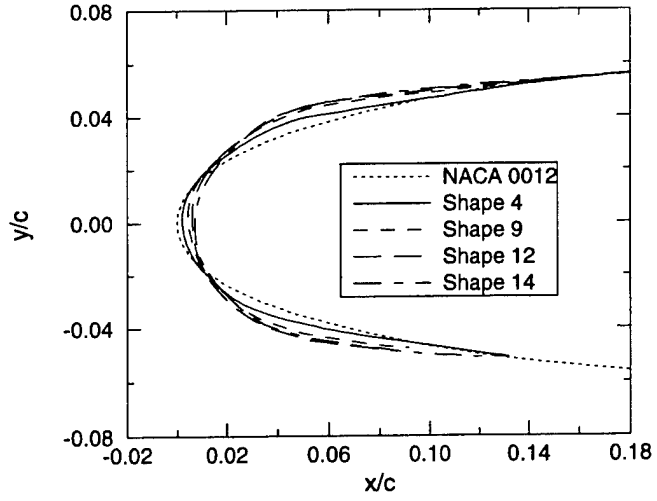

Fig. 7. DDLE Airfoil Shape Profiles.

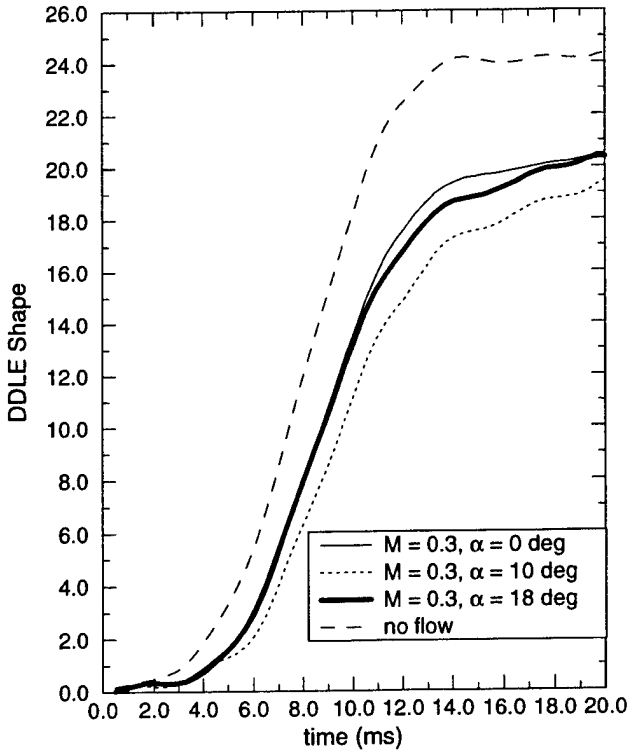

Fig. 9. Effect of Aerodynamic Loads on DDLE Motion History: M = 0.3, V(10).

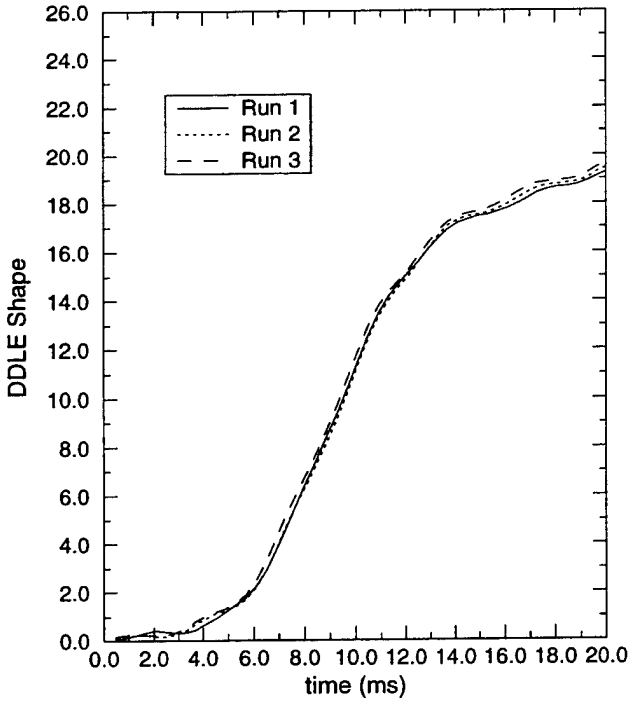

Fig. 8. Repeatability of DDLE Motion History: M = 0.3, k = 0, α = 10 deg, V(10).

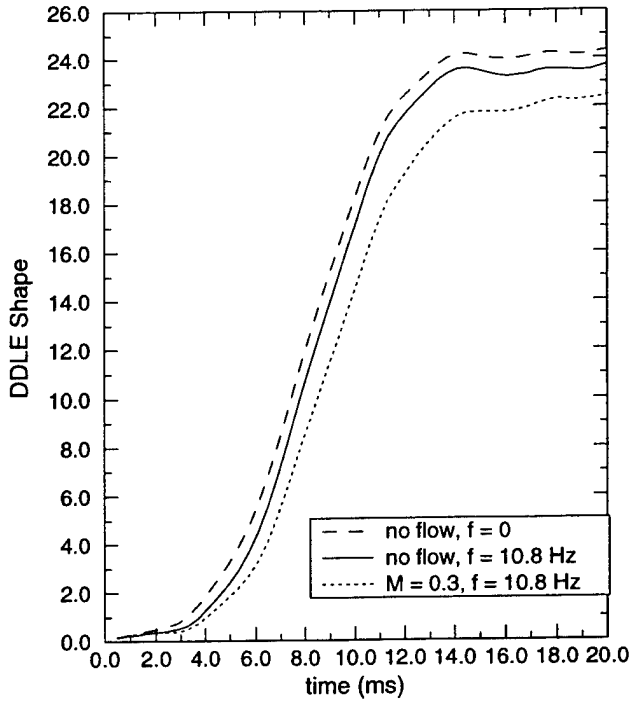

Fig. 10. Effect of Oscillations on DDLE Motion History: V(10).

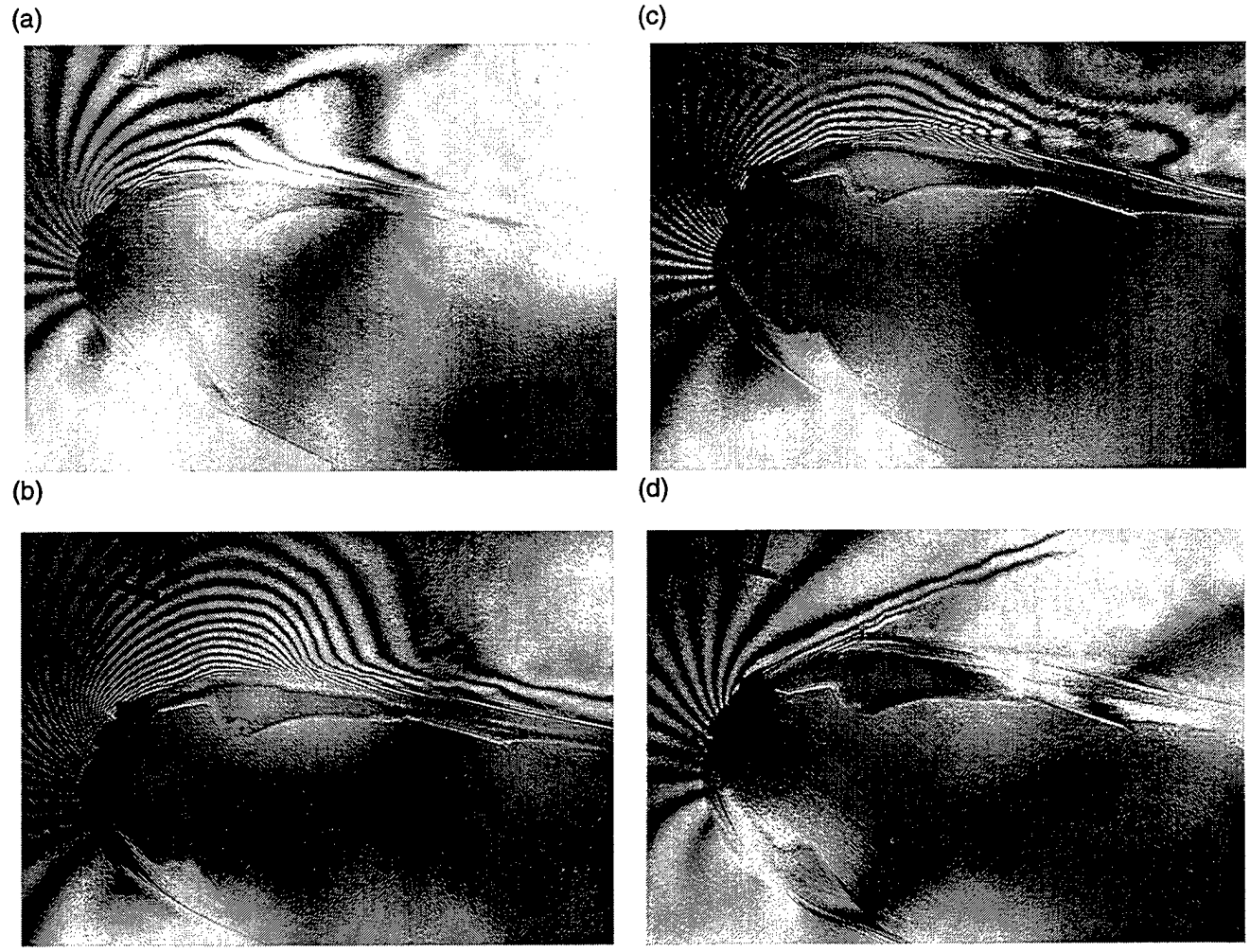

Fig. 11. Flow Modification with Changing Leading Edge Shape: M = 0.3, α = 18.00 deg; (a) Shape 4; (b) Shape 9; (c) Shape 12; (d) Shape 15.

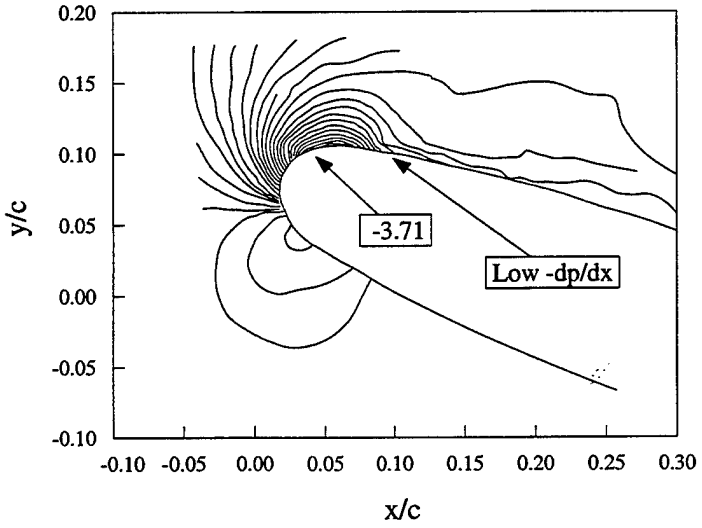

Fig. 12. Global Pressure Distribution over a Shape 8 Airfoil: M = 0.3, k = 0.05, α = 10 deg + 10 deg sin(ωt) = 20.00 deg, upstroke.